Research of a Gas Phase under Electrical Explosion of the Titan Foil in Liquid

Leonid Irbekovich Urutskoev[a,b], Dmitry Vitalievich Filippov[a,b],
Anri Amvrosievich Rukhadze[c], Vadim Pavlovich Bystrov[c], Yury Petrovich Dontsov[d],
Victor Semionovich Parbuzin[e], and Alexandr Vvasilievich Steblevsky[f]

[a] RECOM, National Research Center 'Kurchatov Institute', Moscow, Russia
[b] Moscow State University Of Printing Arts, Moscow, Russia
[c] General Physics Institute (Russian Academy Of Sciences), Moscow, Russia
[d] National Research Center 'Kurchatov Institute', Moscow, Russia
[e] Moscow State University Department of Chemistry, Moscow, Russia
[f] Institute of Inorganic Chemistry, Moscow, Russia

Reprint requests to D. V. F.; E-mail: filippov-atom@ya.ru

Experimental studies of pulsed electric explosion of thin titanium foils in water with discharge power of ~ 0.2 GW are described. The production of a considerable amount of molecular hydrogen is revealed whose origin can be explained neither by water decomposition nor by known chemical reactions. A nuclear mechanism of occurrence of the observed molecular hydrogen upon electric explosion is hypothesized. Emphasis is laid on some measurements confirming the hypothesis.

Key words: Electrical Explosion; Hydrogen.

1. Introduction

It is well known that high power electrical explosions of metallic wires in liquid cause strong magnetic fields ($H \sim 1$ MGs) and high impulse pressures ($P \sim 10^5$ atm) [1,2]. On the other hand, however, there is no doubt that such strong external fields can quite significantly change the probability of nuclear decays and even the conditions of stability of nuclei [3]. So, for instance, the full ^{187}Re ionization leads to a greater probability of β-decay (due to the decay into the electron bound state) [4] while the full ionization of the stable ^{163}Dy, ^{193}Ir, and ^{205}Tl isotopes makes them β-active (the half-decay of the fully ionized ^{163}Dy becomes equal to 47 ± 5 days [5]). It has been theoretically shown that powerful magnetic fields change the probability of β-decays because of changes in the phase space of the final states of appearing β-electrons [6].

Atomic electrons increase the probability of α-decay in relation to the probability of the fully ionized atom α-decay. Firstly, the atomic electrons create the α-particle barrier, and secondly, the α-decay decreases the nuclear charge by two units which results in energy changes of the electron shell. Taking into account that the atomic electrons lead to the result when calculating the α-decay constant, the energy of the α-particle should be replaced by 'effective' energy which is greater than the actual energy: $E \rightarrow E + 73Z^{4/3} + 65Z^{5/3}$ eV [7]. The influence of the said atomic electrons can become quite significant due to the exponential dependence of the probability of α-decay on the α-particle energy $\ln p \propto \text{const} - 1/\sqrt{E}$ [8]. Atomic electrons, as one would expect, exert stronger influence on decays with low energies. For instance, the electron shell of ^{147}Sm (the energy of α-particles ~ 2.31 MeV; $T_{1/2} = 7 \times 10^{11}$ yr) increases the probability of α-decay 2.6 times as compared with the nucleus of a fully ionized atom [7].

Qualitatively, the influence of a superstrong magnetic field on the probability of α-decay can be described as follows: this external superstrong magnetic field changes the energy of the atomic electron shell [9] and therefore the energy of any nuclear decay, because the energy of such a decay equals the difference between the full energies of the initial and the final states of a system, taking into consideration the energies of ionization of atoms or ions [3]. The external superstrong magnetic field leads to a greater energy of decay and, hence, to a greater probability of α-decay. Besides, such an external magnetic field changes the geometry of the problem replacing the spherical symmetry by the allocated direction along the said mag-
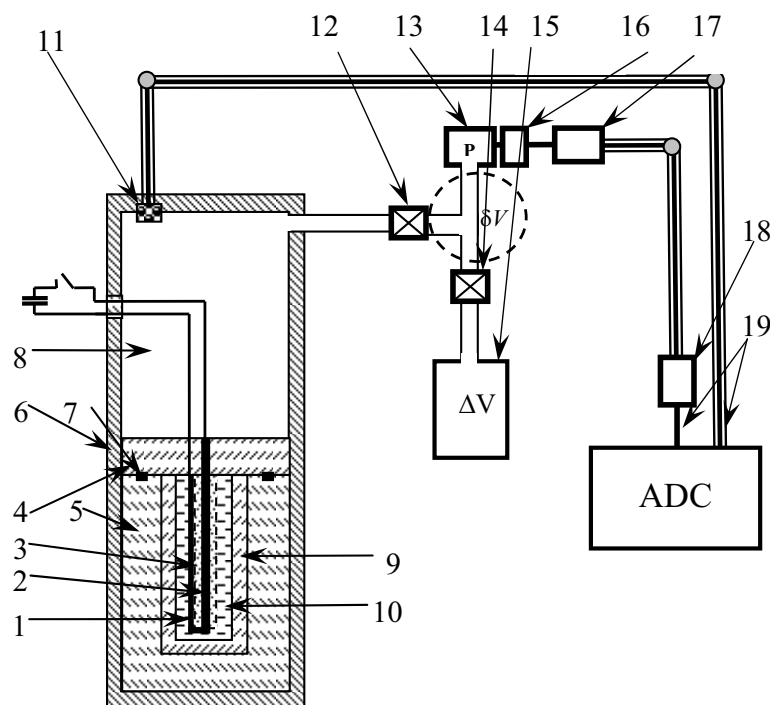
Fig. 1. Schematic drawing of experimental setup.

1 – titanium foil; *2* – titanium electrode; *3* – insulator; *4* – lid; *5* – interior of the explosion chamber; *6* – stainless steel frame; *7* – tightening; *8* – gas-collecting chamber; *9* – disposable beaker; *10* – liquid; *11* – piezoelectric sensor of resultant pressure; *12* – valve; *13* – polarographic sensor DV-16 of hydrogen partial pressure; *14* – valve; *15* – calibrated gas-collecting balloon; *16* – signal amplifier; *17* – voltage-frequency signal transducer; *18* – frequency-voltage signal transducer; *19* – cable.

netic field. This influence ambiguously depends on the magnetic moments of both the initial and the final state of the decomposing nucleus and, in the general case, can result in different signs depending on the strength of the magnetic field.

In this connection, in our previous researches we carefully studied electrical foil explosions in uranium salts [10, 11] in order to detect, experimentally, the ionization and powerful magnetic field influence on changing the β-decay periods. During these experiments we studied the gas phase of such electrical explosions (i. e. the gasses resulting from these explosions). But the analysis of the gas mixture showed an abnormally high content of hydrogen. A thorough investigation of this phenomenon required more than five hundred experiments and took at least about four years. The concrete results of this research are stated briefly in the present article.

2. Description of the Experimental Setup

The experimental setup consisted of two capacitor batteries with $C = 2.5 \times 10^{-3}$ F each. One was charged by $+4.8$ kV, the second by -4.8 kV (relative to the 'earth' potential). Under maximum voltage, the energy reserve was $W \sim 50$ kJ. Two vacuum solid state spark-

gaps of trigatron-type were used as commutators and were commuted by special devices. The current impulse of each battery was $T \sim 120\ \mu$s and it's amplitude was about $I_0 \sim 120$ kA. The current has been measured by coaxial shunts and the voltage by a divider well described in [10, 11], also supplied together with oscillogram data of the electrical current and the voltage. Analogue oscillographs as well as rapid analog-digital transformers attached to computers were used to register electric signals. The time spread of gaps, as a rule, was no more than $\tau = \pm 30 \times 10^{-6}$ s. Transporting an electrical impulse from each battery was done by means of four coaxial cables (the current transported through one cable was $I \sim 30$ kA thus enabling us to preserve its longer mechanical durability). Their induction was $L = 0.4\ \mu$H. Thus, the setup in fact could work with eight independent electrical loads simultaneously. The respective registering equipment was in the shielding room at the distance of ~ 40 m to avoid electromagnetic disturbance.

In the said run of experiments, each battery worked with its own electrical load which was a titan foil *1* (Fig. 1) welded to a massive titan electrode *2* by means of contact electrical welding. Figure 1 graphically shows one of two explosion chambers where a teflon insulator *3* was set between a massive electrode

and a foil to make this foil cable armor connected immediately with the central cable wire. The electrodes were fixed to the dielectric insulator (*4* as shown in the figure) made either of polyethylene or teflon depending on the experiment purpose. Simultaneously, this insulator served as a packing element for the explosion chamber. The mass of the titan foil (loading) varied in different experiments from one to four stripes and each of them was $\Delta = 50$ μm in thickness, 1 cm wide, and $L = 4.0$ cm in length. The mass of every stripe was $m = (90 \pm 5) \times 10^{-3}$ g.

The interior of the explosion chamber *5* was made of polyethylene (or teflon) and placed in the lower part of a firm body made of stainless steel *6* and providing its hermetic state in all the experiments. All the sealing elements were made of non-hydrogenous materials. Hermeticy of the explosion chamber itself was provided by sealing *7* of the lid *4*. The power input was through the upper part of the metallic container at the same time being a $V = 3.125$ ℓ volume gas-collecting chamber *8*. The inside of the explosion chamber *5* contained a disposable glass *9* made of teflon (or polyethylene) which was filled with liquid *10* and the central electrode with foil welded to it. During electrical explosion, glass *9* was subjected to the maximum mechanical deformation and when made of teflon then it was subject to just mechanical destruction. Therefore, practical use of this construction element significantly prolonged the service time of the basic part *5* of the explosion chamber. The volume of the said liquid (in the main part of the experiments) was $\upsilon \sim 18$ cm^3. The liquids used were either de-ionized bi-distillate (H$_2$O) or certified heavy water 99.8 % (D$_2$O). After electric explosion, the pressure in the chamber rapidly increased and the resulting gas broke through the sealing *7* into the gas collector *8*.

The necessity of the gas collector is explained by the fact that no attempts to hold back gases in the explosion chamber have led to any positive result but only to mechanical destruction of the explosion chamber.

There was a pressure gauge in the upper part of the gas collector cylinder *11* and a pipe which, through valve *12*, was connected to the partial hydrogen pressure transducer *13* and, through valve *14*, to the calibrated gas collector (volume *15*, $\Delta V = 250$ cm^3), whose function will be discussed below. Prior to installing, the said gas collecting cylinder had been pumped out down to 2×10^{-2} Torr pressure. At the same time the gas collecting chamber itself, right before the electrical explosion, had been pumped out down to the pressure of several Torr, blown through

with argon several times and then filled in with high quality argon until the pressure became $P = 1.5$ atm. Such a procedure enabled us to minimize the influence of atmospheric gases on the results of further measurements.

3. Description of Measurement Methodology

This research used both the standard methodologies (solid-state laser mass-spectrometry, gas chromatography, gas mass-spectroscopy, electronic microscopy) and methods specially developed for this particular experiment (measuring relative hydrogen content, optical and other methods of making calibrating the hydrogen-deuterium gas mixtures).

3.1. Method of Hydrogen Partial Pressure Measurements

Since the results of measuring the amount of produced hydrogen are of great importance for the present research, this method will be analyzed most thoroughly. The method involved the following measuring means: a sensor of hydrogen partial pressure, a sensor of total pressure, a block of electronics, an analogue-to-digital converter (ADC), and a computer. A polarographic DV-16 sensor (produced by the '*Insovt*' CJSS, Saint-Petersburg) [12] was used as a partial hydrogen pressure sensor. The sensor operation is based on the linear dependence of the diffusion current running in the polarographic cell on the partial pressure of electrolyte-dissolved hydrogen. Our tests showed that the sensor response function depends on two parameters, namely, the hydrogen partial pressure P_H and the total pressure P_0 in the mixture. Note that in the pressure range 1 atm $< P_0 < 2.5$ atm the dependence $U_{PH} = f(P_0)$ is not strong, but a special calibration procedure was needed to heighten the precision of the measurements.

The experimental conditions required information transfer on the measured parameter at a considerable distance (over 30 m), which resulted in overlapping between noise and the useful signal. Furthermore, at the instant of electric explosion, high-voltage discharges are very likely to get onto the hydrogen sensor circuits, which, in the case of galvanic coupling in constant current, can cause failure of the entire measurement system. The problem was solved by converting the measured voltage into frequency. Such technique allows signal transfer over large distances without taking a risk of useful information distortion by noise, induc-
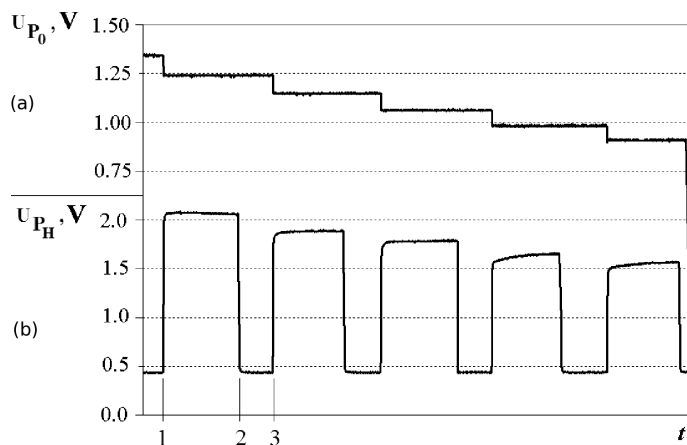
Fig. 2. Signals from pressure (a) and hydrogen pressure (b) sensors.

1 – instant of valve *14* opening (Fig. 1); 1 – 2 – measurement time; 2 – instant of valve *12* closure and balloon *15* and sensor *13* detachment; 2 – 3 – sensor expulsion and balloon pumping-out.

tions, and other changes in the signal amplitude. This approach also allowed us to make a galvanic decoupling of the measuring circuit thanks to a most simply realizable capacitive coupling. The reverse (frequency-to-voltage) conversion unit was placed close to the digitizing unit. The error (nonlinearity) in the signal voltage-to-frequency conversion was ±0.03 %, the error (nonlinearity) of the reverse (frequency-to-voltage) conversion being ±0.06 %, which is much less than the hydrogen meter basic error of ±1.5 %.

A Siemens Sitrans P Serie Z, Typ 7MF 1564 piezoelectric sensor was used to measure the total gas-mixture pressure in the chamber. The electric signal U_{P0} from the sensor was taken directly to the ADC. Linearity of the sensor, along with the whole tract, was verified by a standard manometer. The calibration showed that the measuring system is linear with good approximation up to ~ 0.1 %, which is even higher than guaranteed by the producer.

After an electric explosion of the foil, the pressure in the gas-collecting chamber became $P_0 \sim 2$ atm and was controlled by the pressure sensor *11* (Fig. 1). At the instant of 'shot' the valve *12* was shut off, which was dictated by the exploitation characteristics of the hydrogen sensor. Because the latter lost operability upon both a sharp pressure jump and a forevacuum evacuation. The valve *14* was also closed and cut off the calibrated balloon *15* from the chamber working volume. The use of the calibrated balloon *15* is needed within this method because the air occurring between the valves *12*, *14*, and the pressure sensor *13* (see Fig. 1) cannot be pumped out of the 'ballast' volume $\delta V \sim 18$ cm^3. Thus, the ballast volume δV turned out to be filled with air at atmospheric pressure. This

was responsible for the fact that after the valve *12* was opened, partial equilibrium between the measured gas volume V_0 and the hydrogen sensor set in very slowly because of the low diffusion rate through the membrane. One measurement, therefore, took up much time.

The measuring procedure was as follows. To decrease the time within which stationary regime of pressure measurements is established, the valve *14* was opened and the gas was 'pressed' into the volume V. In such a measuring procedure, the stationary regime was established in the hydrogen partial pressure sensor within only ~ 30 min. Figure 2 demonstrates signals from the pressure sensor *a* and the hydrogen sensor *b*, registered by ADC in the course of measurement. The figure shows that at the moment when the valve *14* is opened, the sensor 13 shows a sharp jump up (step 1 in Fig. 2b). At this instant, the total-pressure sensor shows a jump-like pressure lowering (Fig. 2a). Next, the valve to the hydrogen-pressure sensor is closed (step 2 in Fig. 2), and the calibration balloon and the hydrogen sensor are detached. The calibration balloon is again pumped out to a vacuum of 10^{-2} Torr, and then the partial pressure is measured several times.

Assuming the process to be isothermal, we can readily write the relations between the pressures of the *i*th and the $(i+1)$th iteration steps:

$$
\begin{aligned}
P_0^i &= P_0^{i+1}\left(\frac{V_0 + \Delta V}{V_0}\right) + \frac{\delta V}{V_0}(P_0^{i+1} - P_a), \\
P_H^i &= P_H^{i+1}\left(\frac{v_0 + \Delta V + \delta V}{V_0}\right),
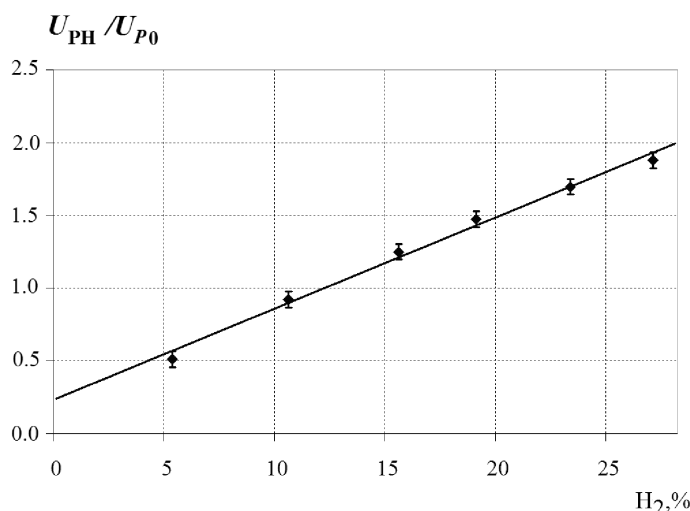\end{aligned}
\tag{1}
$$

U_{PH}/U_{P0}

Fig. 3. Result of method calibration.

where P is the pressure in atmospheres and $P_a = 1$ atm is atmospheric pressure.

Since at each step the relative hydrogen content depends on the initial relative hydrogen content γ^0 and the known volumes

$$\gamma^{i+1} = \frac{P_H^{i+1}}{P_0^{i+1}} = \gamma^i \left(1 + \frac{P_a \delta V}{P_0^i V_0}\right)^{-1}, \qquad (2)$$

we obtain n measurements of one and the same quantity γ^0. The advantage of such a method lies in the decrease, due to averaging, of the measurement error caused by the weak dependence of the readings of the hydrogen partial pressure sensor on the total gas-mixture pressure P_0. If the parameter $\delta V/V_0 \sim 0.6\% \ll 1$ is neglected then $\gamma^i = \gamma^0$, and the computational formulas are notably simplified. To make sure that the method works well, we prepared a calibration mixture (83 % of Ar + 17 % of H_2). The hydrogen concentration was measured by the above-described method with a no less than one percent error.

To make certain that the elaborated method of hydrogen percentage measurement is linear in the concentration range of interest, we prepared $(Ar + H_2)$ mixtures of different concentrations. The calibration mixture composition was controlled using a gas chromatograph.

Figure 3 presents the results of calibration for gas mixtures with different relative contents of hydrogen. The hydrogen percentage in the mixture is plotted on the abscissa axis, and the dimensionless ratio $\langle U_{PH} \rangle / \langle U_{P0} \rangle$ averaged over the steps is plotted on the ordinate. One can see in the figure that within the range

$5\% < \gamma < 30\%$ the response function is linear depending on γ.

Our method also made it possible to measure slow variations of relative hydrogen content during several days. The method is insensitive to the replacement of H_2 by D_2 or HD.

Using this method, we measured to a high accuracy the gas-collecting chamber volume which we had to know for a correct calculation of absolute amounts of gases due to electric explosion.

3.2. Method of Chromatographic Analysis

Gas chromatography was used, on the one hand, to control the above described method for determining the specific hydrogen content in the gas mixture under study and, on the other hand, to perform a qualitative and quantitative analysis of the gas mixture. We used a gas chromatograph LCM-80 which included three sorption columns. The analysis was carried out at a temperature of 40 °C in isothermal regime. Using the sampling system (balloon 15 of Fig. 1) the gas products of the process were taken in plastic bags. The gas sample at atmospheric pressure was introduced into each column separately using either a gas syringe or a dosimeter valve. The volume of the introduced sample was $0.5 - 1$ mℓ. The analyzed mixture components were registered by a detector based on measurements of thermal conductivity of separate gas-mixture components. The quantitative composition of the gas mixture was calculated by the absolute calibration method by chromatographic peak areas (for gaseous components CH_4, C_2H_4, C_2H_2, and CO_2).

Standard gas mixtures were used for calibration with respect to hydrogen, nitrogen, and CO. We either made calibration the same day as the gas samples were tested or used the calibration of the previous analysis. Since the measured hydrogen, nitrogen, and carbon monoxide concentrations were in the range of calibration gas mixtures, we used linear interpolation in height to calculate tested component concentrations. The method did not permit measurement of hydrogen isotopic distribution.

3.3. Method of Solid-State Laser Mass Spectrometry

We have used laser mass spectrometry here only to determine the degree of oxidation of titanium powder appearing from the foil as a result of explosion. This information was necessary for the correct account of the amount of oxygen absorbed by titanium. In other words, the method was aimed at determining the n value in the TiO_n formula in each experiment. In addition, we were interested in the isotopic distribution of titanium contained in the powder. Therefore, to determine the element and isotope compositions of the liquid and metal foil remainders we chose laser mass-spectrometry which, given sufficient sensitivity $(10^{-4} - 10^{-5}$ at. %), shows an error of $10 - 15$ % in determining the amount of micro-impurities.

The method was based on the 'EMAL-2' laser mass-spectrometer designed for element analysis of solid samples. This device had been used in our previous research for many years and was described in sufficient detail in the works published earlier [10, 11, 13]. We have also repeatedly tested the results through other type mass-spectrometers never finding any obvious contradictions. Hence, it was the only method in this research that could work without any alternative approaches. Nevertheless, validity of the measurements has permanently been checked through both the standard alloy samples and certified geological ones.

3.4. Method of Gas Mass-Spectrometry

Gas mass-spectrometry played two parts in our research. On the one hand, it duplicated the gas chromatographer measurements, and therefore, when extracted from the same removable containers and already measured on the gas chromatograph, the gas was examined using the gas mass-spectrometer. On the other hand, this method was very important for finding the isotopic distribution of hydrogen atoms in the gas

mixture due to electric explosion in experiments with liquid represented by 'heavy water'.

The method rested upon a time-of-flight quadrupole unipolar mass-spectrometer MMC-1A described in greater detail in [13], which allowed components to be determined within the 1 to 400 atomic mass range. The gas sample composition was tested by mass spectrometry on a superhigh-vacuum test stand in dynamic regime. The initial test volume pressure of no more than 10^{-8} Torr was reached through heating under pump-out condition. The gas was let into the test volume through a leak in the throttling regime up to a pressure of 4×10^{-6} Torr. The test with etalon gas mixtures showed that this method had no less than 5 % error in the entire mass range of interest. In some cases, to check correctness of measurement correlations for the 2nd, 3rd, and 4th masses (H_2, HD, D_2) we used gas mass-spectrometer with magnetic focusing. The obtained results showed good agreement. Masses over the 44th (CO_2) were not observed in the tested gas samples to within 5 % precision.

3.5. Spectral Analysis

Optical spectroscopy was chosen as a duplicate method for a qualitative element and semi-quantitative isotopic analysis of hydrogen. For this purpose, a special setup was designed shown schematically in Figure 4. This setup made it possible to obtain and investigate the radiation spectrum of high-frequency discharge occurring in the gas flow. The optical spectrum was investigated through a quartz discharge tube joined to the glass part of the vacuum unit with a specially made quartz-glass connector. The metallic details were
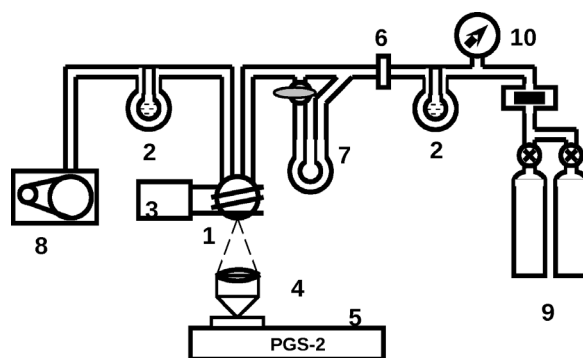

Fig. 4. Schematic of optical device.

1 – quartz volume; *2* – nitrogen trap; *3* – high-frequency generator; *4* – lens; *5* – spectrograph; *6* – inlet tap; *7* – oil manometer; *8* – fore-vacuum pump; *9* – investigated balloons; *10* – pointer manometer.

attached to the setup by kovar-glass sleeve. Vacuum rubber fills were only used where gas containers were attached to the analytical system and also where the setup was joined to the forevacuum pump.

The basic characteristic of the described analytical setup is the fact that the most probable gas pollution (rubber, vacuum lubricants in the valves) sources are removed rather far from the discharge region *1* (Fig. 4). Traps with liquid nitrogen *2* which froze out vapors from water-containing liquids were placed with the same purpose in front of and behind the discharge region. These liquids are normally contained in forevacuum pump oil, the vacuum-valve lubricant, and can get into the gas balloon when a gas sample is taken from the experimental setup. To avoid accumulation in the high-frequency discharge region of impurities which could be due to different microcracks and glass degassing, the discharge was realized in the gas flow. The maximum pressure of the remaining gas in the setup volume was nearly 10^{-3} Torr, while the gas flow pressure during the discharge was ~ 3.0 Torr. We shall see below that these measurements sufficed to avoid alien impurities in the gas under investigation.

The gas was excited in a gas tube *1* (see Fig. 4) with a high-frequency Tesla generator *3*. The occurring optical radiation was gathered by a quartz objective *4* and focused on $1 : 1$ scale onto the slit *5* of the spectrograph with diffraction grating (PGS-2). The dispersion of the device in the area under study was 7.3 Å/mm. The 3000 Å to 5000 Å spectral range was photographed on a 1300-unit sensitivity RF-3 fluorographic film and in the 5000 Å to 7000 Å range – on a 1800 State Standard aerofilm.

As has been mentioned above, the main goal of the optical spectral method was the relative measurement of H and D atom concentration in the gas mixture composition. The optical method coped well with this task and, moreover, yielded many quite unexpected results. But their detailed presentation would take too much space and lead the reader away from the main facts brought in here.

4. Experimental Results

4.1. Basic Results

As has been said above, ionized gas is produced at the instant of foil electric explosion, which breaks through the fills from the explosion chamber to the fore-chamber. For constant parameters of the experi-

Table 1. Characteristic times of pressure measurements, s.

ADC-1 (MHz)	ADC-2 (Hz)
	0.04
0.366 ± 0.004	0.379 ± 0.003
3.8	

ment, namely, load mass, foil type, explosion chamber geometry, type of liquid, magnitude of current, etc., the pressure jump shows one and the same value. For example, for the Ti load mass $m_{Ti} = 180$ mg the pressure jump was $\Delta P = 0.42 \pm 0.04$ atm which, when recalculated for the chamber volume, made up $\Delta N = 3.4 \times 10^{22}$ atoms. At first glance, this result may seem to be absolutely natural because it is common knowledge that an electric charge running through water must generate hydrogen and oxygen. But it should be taken into account that an electric charge stored in a capacitor bank amounted to $Q \sim 11$ C and the Faraday number is $F \sim 96500$ C/mole.

Note that the reproducibility of the effect in these experiments on many factors which at first glance may seem insignificant. However, it took us about two years to attain satisfactory reproducibility of the results.

As has already been said above, when the capacitor bank was actuated, currents and voltages under electric load and signals from the piezoelectric pressure sensor were registered. The signal from the pressure sensor branched consistently and then was digitized through two different analogue-to-digital converters (ADC). The signal digitization frequency was $\nu = 0.2$ MHz for the first ('fast') ADC signal and $\nu = 10$ Hz for the second ('slow') ADC. Typical signals from both ADCs are illustrated in Figure 5. Each of the signals is well approximated by the two exponents:

$$P(t) = y_0 + A_1 \exp\left(\frac{t - t_0}{t_1}\right) + A_2 \exp\left(\frac{t - t_0}{t_2}\right). \quad (3)$$

The t_1 and t_2 values are given in Table 1.

The characteristic exponent periods for the first signal are $T_1 \sim 40$ ms and $T_2 \sim 0.3$ s and for the second signal $T_2 \sim 0.3$ s and $T_3 \sim 3.2$ s. One can thus see that the pressure behaviour in time is characterized by three scales. This issue has not been thoroughly studied here, but we may assume the first exponent period $T_1 \sim 40$ ms to be due to radiative cooling, the second one $T_2 \sim 0.3$ s – to transition gas-dynamical processes, and the third period $T_3 \sim 3.2$ s – to heat conductivity. The amplification rate and the amplitude of the signal in Figure 5a were indicative, although quite indirectly,
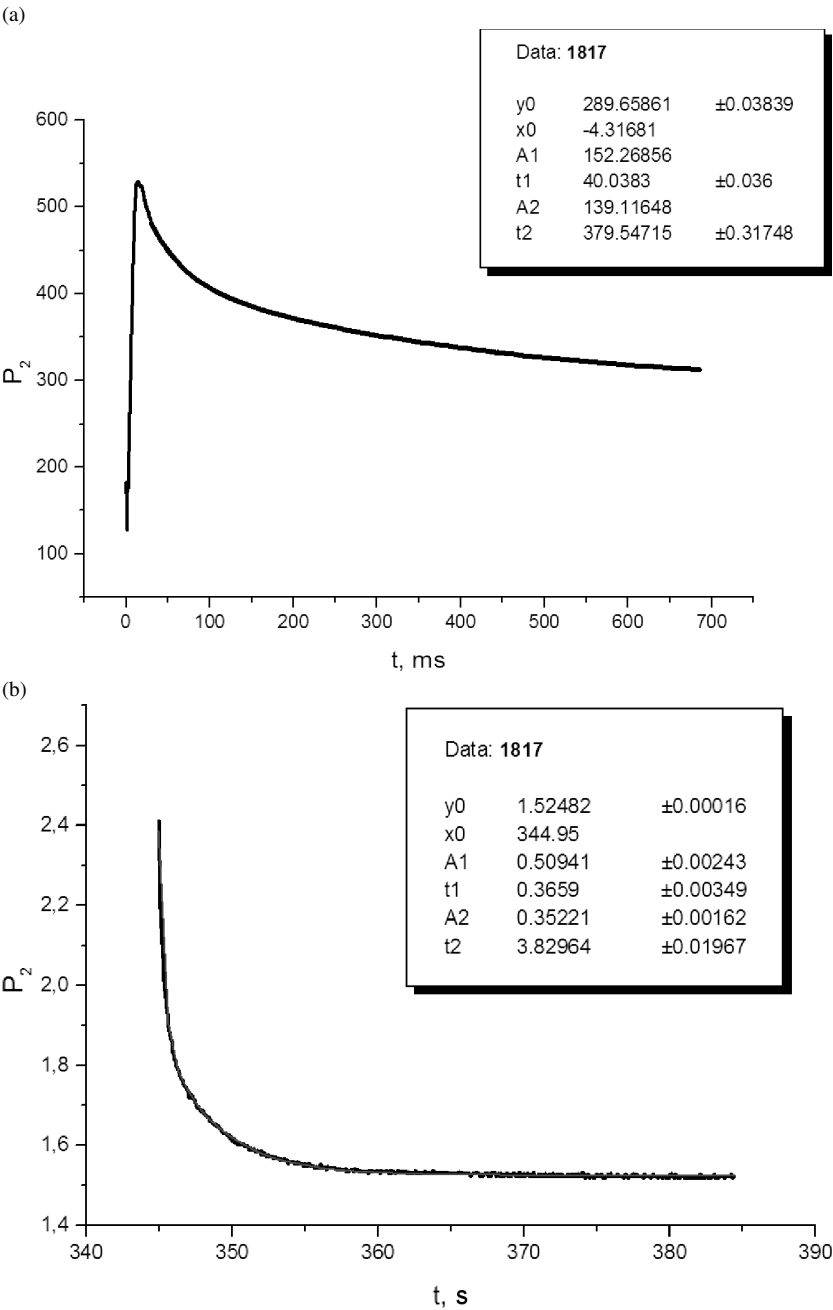
(a)

Data: **1817**

y0	289.65861	±0.03839
x0	-4.31681	
A1	152.26856	
t1	40.0383	±0.036
A2	139.11648	
t2	379.54715	±0.31748

(b)

Data: **1817**

y0	1.52482	±0.00016
x0	344.95	
A1	0.50941	±0.00243
t1	0.3659	±0.00349
A2	0.35221	±0.00162
t2	3.82964	±0.01967

Fig. 5. Signal from fast ADC (a) and from slow ADC (b).

of the gas gain intensity. And the signal from the slow ADC (Fig. 5b) made it possible to control the chamber hermiticity after the 'shot' and the hydrogen partial pressure measurement (see Fig. 2b). Figure 5b shows that in 20–30 s after an electrical pulse all transition processes mainly terminate and the pressure becomes stationary.

At the early stage of our present research the main effort was directed to investigate the chemical composition of the gas formed upon a titanium foil electric explosion. In several minutes after the explosion, i. e., when the pressure and temperature in the gas-collecting chamber have already reached their stationary values, the hydrogen partial pressure in the pro-
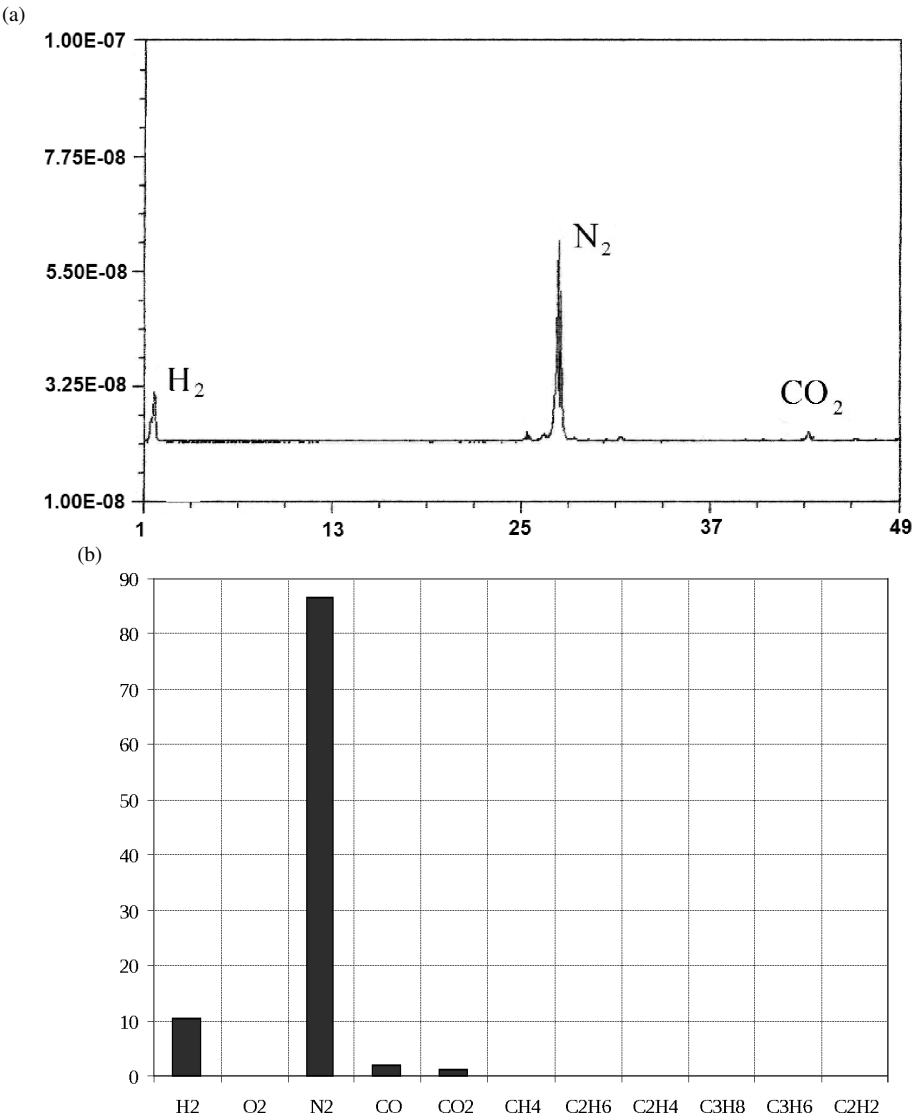
(a)

(b)

Fig. 6. Gas mass-spectrum (a) and gas chromatography (b).

Table 2. Typical result of gas chromatograph measurements.

Element	%	Element	%	Element	%
H_2	13.97	O_2	< 0.3	N_2	0.6
CO	3.62	Ar	80.85	CO_2	0.4
CH_4	< 0.02	C_2H_6	< 0.03	C_2H_4	< 0.04
C_3H_8	< 0.1	C_3H_6	< 0.1	C_2H_2	< 0.07
		Σ	100		

duced gas mixture was measured by the method described above. After that, the gas was sampled to a calibration balloon and analyzed using gas chromatograph. Table 2 presents a typical gas chronometer measurement. The table shows that the basic component, except argon as a ballast gas, is hydrogen. One can no-

tice the absence of oxygen beyond the method sensitivity limits.

Table 3 gives a comparison of the values of measured relative H_2 content in the gas mixture, obtained with gas chromatograph and polarization sensor for one series of experiments, where Ar was also used as buffer gas. We note that the buffer argon chemical 'purity' was 99.8 %. The table demonstrates a good coincidence of the results obtained by two different methods. And, nevertheless, to make sure that the gas chromatograph yields a correct chemical composition of the mixture, part of gas samples was simultaneously analyzed using gas mass-spectrometer. Figure 6 gives

Table 3. Measured values of relative hydrogen content obtained using gas chromatograph of polarization sensor for the series of experiments with loading $m_{Ti} = 180$ mg.

No.	1830		1829		1828		1826	1825	1824	1823	1822	average
Polarogr.	15.76	16.89	14.2	14.0	17.9	19.5	16.8	13.4	14.4	15.6	18.5	**16.1 ± 2**
Gas. chrom.	17.4	15.4	16.4	14.1	18.5	16.8	16.4	12.8	13.7	14.5	18.0	**15.8 ± 1.8**

the results of analysis of one of the samples obtained using the gas mass-spectrometer (Fig. 6a) and the gas chromatograph (Fig. 6b) for the case when N_2 of high chemical purity was used as buffer gas. The figure demonstrates good qualitative agreement of the two methods. In Figure 6a one can see that the gas mass-spectrometer also shows (within the method sensitivity) the absence of free oxygen.

Coincidence of the results of measurements taken within different methods implies that the anomalously large amount of hydrogen and the absence of oxygen are not due to erroneous measurements. Simple recalculation of the relative hydrogen content with allowance for the chamber volume and the total pressure shows that during a pulse $\sim 0.9\,\ell$ of hydrogen is generated (under normal conditions) in each chamber. This result is rather stable, reliable, and verified in a large number of experiments. Thus, if we assume that the registered hydrogen is a result of chemical or pyrolytic water decomposition, the question arises: Where did the oxygen disappear? In other words, $0.9\,\ell$ of atomic oxygen due to water decomposition must have been absorbed by the chamber surface without producing a notable amount of molecular oxygen. And as follows from Figure 5b, this mechanism must be actuated within the first seconds because after that the pressure lowering stops.

4.2. Analysis of the Chemical Mechanism of Hydrogen Production

To try and examine the physical mechanism of hydrogen production, it was necessary to establish balance in oxygen. An insignificant part of oxygen was found in the gas sample in the form of CO and CO_2, and this amount of oxygen could readily be taken into account in the general balance. The reason for the absence of free oxygen could be oxidation of the titanium electrode and exploded foil. Neither titanium electrode isolation from water, using teflon, nor the change of Ti electrodes by electrodes made of metals possessing lower oxidability (stainless steel, cobalt, etc.) has led to observation of oxygen in the generated gas.

As concerns titanium foil oxidation, this channel of oxygen binding was allowed for by the solid-state mass spectrometry method. To this end, we examined the foil remainders and measured the Ti/O ratio. As a result of numerous measurements it was found that titanium oxidizes to the formula TiO_n ($n = 1.4 \pm 0.2$). This means that part of Ti oxidizes to TiO_2 and part – to TiO. It is worthy of notice that the degree of titanium oxidation depends on the mass of applied load, and this fact was also taken into account in the general balance in oxygen.

For example, for the load mass $m = 180$ mg, one gram-mole of H_2O yields $(2.3 \pm 0.16) \times 10^{22}$ of H_2 molecules upon electric explosion. $N_{O2} = (8.7 \pm 0.9) \times 10^{21}$ oxygen atoms were found in the gas samples in the form of CO and CO_2. The origin of these molecules may well be explained by pyrolytic water-molecule decomposition with a consequent carbon oxide formation due to composition of oxygen atoms with carbon contained, e. g., in polyethylene. When oxidized, the titanium foil binds $N_{O2} = (3.3 \pm 0.6) \times 10^{21}$ atoms. Hence, the oxygen balance fails almost by half, i. e., almost $0.5\,\ell$ of hydrogen does not meet corresponding oxygen atoms.

We have analyzed the dependence of hydrogen output on the titanium foil mass. A series of no less than seven experiments was carried out for each foil mass, and the averaged results are presented in Figure 7. The triangular points refer to the total amount of registered hydrogen, and the round points are for hydrogen of non-chemical origin. The values of standard deviation smaller than the point size were not plotted. In view of the pulsed character of the process the reproducibility of our experiments can be thought of as satisfactory. The figure shows that the amount of non-chemically produced hydrogen does not virtually depend on the titanium foil mass. Noteworthy is the fact that when averaged, the standard deviation values for the lower points appeared to be smaller than those for the initial measurements of the total amount of hydrogen (i. e., for the upper points). Furthermore, the number of hydrogen molecules due to a non-chemical mechanism is $N = 10^{22}$ to a good accuracy irrespective of the foil mass. In other words, this mechanism is more re-
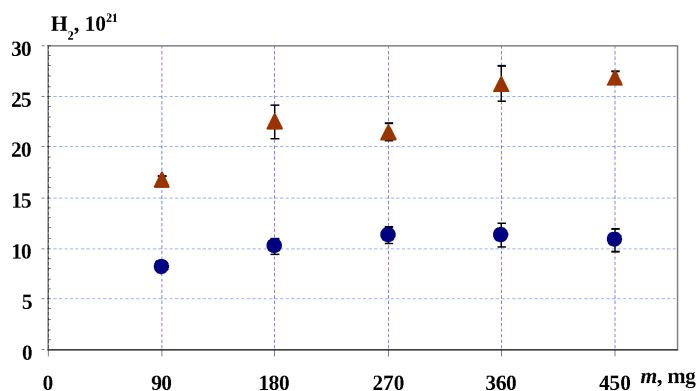
Fig. 7. Dependence of the amount of hydrogen on the foil mass: triangles – registered amount of hydrogen, circles – amount of hydrogen whose origin cannot be explained by the chemical or pyrolytic mechanism of production.

producible and so-to-say 'fundamental' than the foil chemical oxidation. We find it difficult to name the reason for the considerable 'drop' of the upper point for the mass $m = 270$ mg. This was either some systematic carelessness we allowed ourselves in preparation of this series of experiments, or merely a freak of statistics.

The disbalance in oxygen cannot of course be a strong argument for drawing conclusions, but it was a stimulus for seeking the mechanism of 'impurity' hydrogen origin.

4.3. Search for 'Impurity' Hydrogen Sources

4.3.1 Titanium Foil

The titanium foil used in the experiments was the first to be tested as 'impurity'-hydrogen generator. It is common knowledge that titanium can be saturated with hydrogen to the ratio of almost $1:1$. However, most physicists unfortunately forget that this can only be achieved through titanium heating to a high temperature in hydrogen atmosphere. Although spontaneous titanium saturation with hydrogen seems to be improbable, we have nevertheless verified such a possibility experimentally.

To this end, a quadrupole gas mass-spectrometer was used to assemble an experimental stand shown schematically in Figure 8. Since this stand was also exploited for other experiments, whose results are given below, we shall right now describe the measuring procedure in detail so that we might refer to this description later.

The sample-heating device was assembled specially for this experiment. It includes a small heatproof ceramic crucible *1*, a holder, and a heater *2*. The holder

and heater were made of tungsten wire 0.7 mm in diameter. The heater had the shape of a 10-turn cylindrical helix with diameter of 5 mm and step of 0.5 mm spiral.

The foil (or powder) *3* filled about 1/3 of the crucible. The helix was immersed into the crucible down to nearly 3 mm from the foil surface so that the upper heater (spiral) surface could be seen through the optical window.

The measuring procedure was as follows.

1. The background experiment was aimed at measuring the absolute amount and chemical composition of all the impurities contained in both the vacuum system and the crucible itself. For this purpose, an empty crucible was placed in the tested volume (73 ℓ), and the entire volume was pumped out for 15 hours to a pressure of 2×10^{-7} Torr without preliminary heating. Then the pumping was stopped and the background gas separation which normally made up $\sim 2 \times 10^{-6}$ ℓTorr/s.

Then a 320-W heater was switched on, and the temperature measured by its glow exceeded 1600 °C. The pressure rose to $P = 5 \times 10^{-3}$ Torr within 5 min and then got stabilized. After pressure stabilization the heater was turned off, which left the bulk pressure practically unchanged. Thus, knowing the volume and the pressure one can calculate the total amount of desorbed background particles.

To measure the chemical composition of the background gas, the gas was pumped over from the test volume *4* into the pumped-out accumulative volume *5*. Then the tested volume was again pumped out to the background pressure and the investigated gas was pumped into it in doses from the accumulative volume for a consequent mass spectrometric analysis. To gain statistics, we repeated the operation several times. The

Table 4. Composition of gas, released from original foil and powder sediment.

Object of measurement	Number of molecules H_2/g	Composition, %/particle				
		H_2	H_2O	CO	CO_2	other
Background	–	–	5 %	20 %	20 %	10 %
Foil	10^{19}	23 %	24 %	24 %	26 %	3 %
Powder	5×10^{20}	75 %	20 %	5 %	–	–
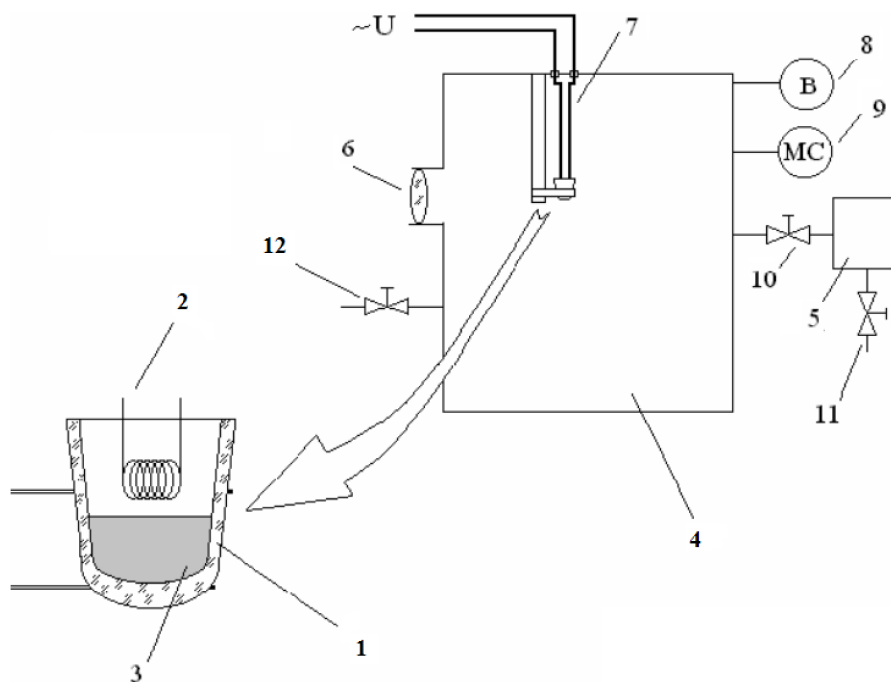
Fig. 8. Schematic drawing of experimental device for examination of gas composition.

1 – crucible; *2* – heater; *3* – investigated material; *4* – tested volume; *5* – accumulative volume; *6* – window; *7* – current feeders; *8* – vacuometer; *9* – massspectrometer; *10* – spill valve; *11, 12* – vacuum pumping-out valve.

results of the mass analysis given in the upper row of Table 4 show that metal-'diluted' hydrogen is absent and the contamination has a surface character.

2. To measure the absolute number of particles and the chemical composition of the gas present in the foil, ~ 0.15 g of cut foil was placed in the crucible. After that a procedure analogous to the above-described one was used to measure the gas contain in the initial titanium foil. After the crucible was heated, the pressure in the accumulative volume was $P \sim 2.5 \times 10^{-2}$ Torr or $N \sim 10^{19}$ atoms per gram of foil (see Table 4). The analysis of the measurement results of the qualitative composition and the amount of gas impurities suggests that the gases contained in the initial foil are impurities located for the most part on or near the surface rather than in the volume.

Thus, the results presented imply that the experimentally observed anomalous amount of hydrogen cannot be explained by its presence in the initial foil.

4.3.2 Polyethylene

Polyethylene contained in the constructional elements of the explosion chamber could have been another probable source of hydrogen. To check validity of such an assumption, all the polyethylene-containing constructional elements inside the hermetical chamber frame were replaced by those made of teflon. We conducted several series of experiments with all other experimental conditions (foil mass, the amount of water, ballast gas pressure, etc.) equal. The experiments gave the following result: the hydrogen content was (16.1 ± 2.2) % in the 'polyethylene' surrounding and (14.0 ± 0.6) % for the 'teflon'. This showed that the polyethylene elements of the explosion chamber construction were not the source of the observed hydrogen. The small difference in the hydrogen percentage was certainly insufficient to explain the registered amount of hydrogen. Hence, even if polyethylene is the source of hydrogen, it is responsible for very small amounts.

It should be noted that when made of teflon, the disposable beaker 9 (Fig. 1) failed to hold high pressure due to electric explosion in the chamber and was destructed, thus increasing the explosion chamber radius. And we shall see below that the diameter of the inner beaker has a very notable effect on the amount of produced hydrogen. When the entire lower part of the explosion chamber (i. e., elements 5 and 9 in Fig. 1) was made of an integral piece of teflon (as an integral constructional element), the difference between two series of experiments in the amount of produced hydrogen was quite insignificant. Thus, our tests seemed on the one hand to heighten the physical intrigue: What is the source of such an amount of hydrogen? And on the other hand they destroyed the hopes for the prospects of creating a simple and inexpensive polyethylene utilization technology.

4.3.3 Other Sources

To finally exclude the hypothesis of 'impurity' origin of hydrogen, we undertook the following series of experiments. We increased the inner beaker (9, Fig. 1) diameter, which was typically 20 mm, and accordingly the exploited bidiscillate volume. All the other construction parts were left unchanged. Dielectric polyethylene details were used. The foil mass remained the same in the entire series of experiments. The percentage of produced hydrogen for different inner beaker diameters is shown in Figure 9. With increasing beaker diameter the explosion chamber pressure falls, which is obviously the reason for the sharp decrease in the amount of produced hydrogen. The last column of the hystogram shows what hydrogen percentage can be due to titanium oxidation and to al-
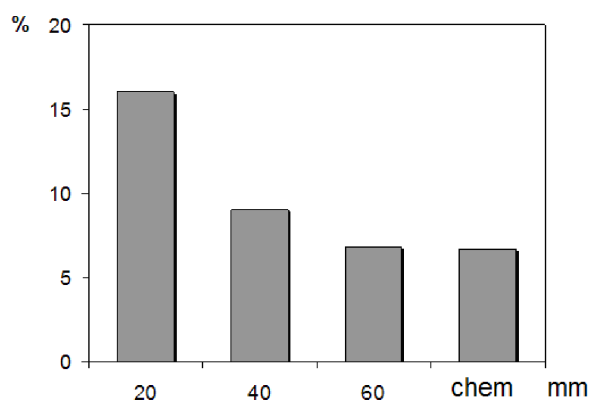

Fig. 9. Percentage of produced hydrogen for different internal diameters of the beaker.

lowance for CO and CO_2 gases. In other words, what amount of hydrogen has a clear chemical origin. All the values in the hystogram have an almost $\sigma_m \sim 1\%$ mean error. The figure shows that with an increase in the beaker diameter up to 40 mm the entire observed hydrogen can already be thought of as having a chemical origin.

All the results presented above suggest that the hydrogen produced at the moment of electric explosion is due to a process yet unknown to us, and its origin cannot be explained by the chemical or 'impurity' mechanism. We believe that the observed hydrogen is of nuclear origin.

4.4. Verification of the Nuclear Hypothesis

To verify the hypothesis, we conducted experiments using 'heavy' water (D_2O) instead of bidiscillate. We used water containing 99.8% of D_2O. The pressure jump and the measured hydrogen percentage differed insignificantly from the experiments with ordinary water. This circumstance suggests that at the moment of electric explosion all processes proceed almost identically in both cases. The idea of experiments with heavy water was as follows. If part of the hydrogen is of nuclear origin, it will not change upon replacement of H by D. Thus, the problem was reduced to determination in a gas sample of a relative H and D content in the produced mixture. We note that the experiments with heavy water were carried out exclusively in a teflon explosion chamber, all the sample intakes were preliminarily pumped out carefully, and the walls were heated to exclude the presence of moist on them.

To solve this problem, we used two methods, namely, optical spectrometry and gas mas-spectrometry. To verify the optical method, we first prepared a gas calibration mixture containing 94% of D and 6% of H. Using the above-described optical method, we measured the ratio of intensities H_α and D_α as well as H_β and D_β for calibration mixture to obtained the values of 95% of D and 5% of H.

A fragment of the calibration optical spectrum is presented in Figure 10a. Such good agreement between the results of optical measurements with the hydrogen concentration values in the calibration mixture means that the optical setup itself contains no 'impurity' hydrogen sources. So, we have made sure that the optical method is correct. Figure 10b shows as an example a fragment of the optical spectrum of the investigated gas mixture. The hydrogen-to-deuterium ratio

(a)

λ_{n} = 6561,32 A λ_{H} = 6562,8 A
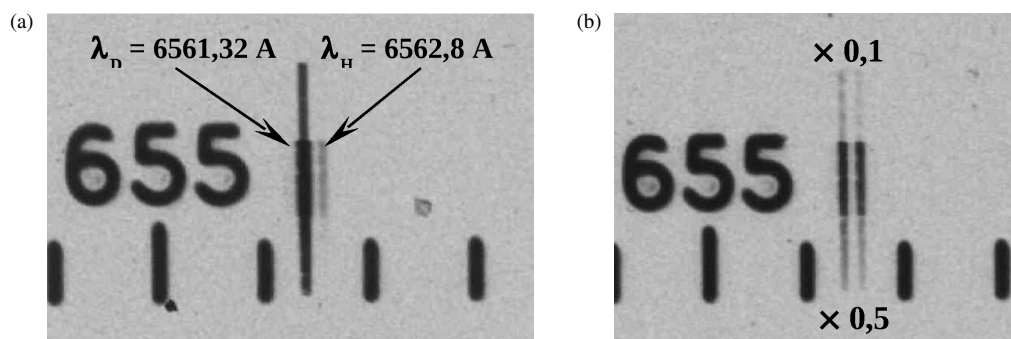
(b)

Fig. 10. Fragment of the optical spectrum taken with depressions of 10 % and 50 %: (a) control; (b) experiment.

measured in this experiment from the optical line ratio made up D/H = 2/1. Approximately the same D-to-H ratio was obtained for this experiment using a gas mass analyzer: D_2/HD/H_2 = 0.5/0.25/0.25.

It is however noteworthy that in a number of measurements taken by the optical method the intensity of deuterium optical lines exceeded the intensity of hydrogen lines, while for other experiments the situation was opposite, which showed that the number of hydrogen atoms exceeded that of deuterium contained in the gas sample. The gas mass-spectrometry gave qualitatively exactly the same results in measurements of the hydrogen isotope composition. Moreover, gas samples taken from the gas-collecting chamber could give different isotopic distributions of hydrogen in different time intervals after the beginning of the experiment. But in the test measurements on sample calibration mixtures, which preceded the measurements of mixtures under study, both the methods gave correct values of isotopic distribution of hydrogen.

It turned out that the gas mixture due to electric explosion was changing its physical properties within several first days. This change was especially notable in measurements on the optical device. If we tried to obtain the gas-mixture optical spectrum at the day of experiment, it was a very difficult task because we either failed to ignite a high-frequency gas discharge at all or its burning was very unstable. The first two days after the experiment the gas mixture exhibited properties of a strongly electronegative gas. While some additional measures helped us to initiate a high-frequency discharge, optical transitions of hydrogen (of all its isotopes) were excited with great difficulty, and we observed for the most part the optical lines of argon. After several days this effect disappeared, and the intensity of all optical lines became comparable with that of the calibration mixture which contained

20 % of (H_2 + D_2) + 80 % of Ar. This corresponded quite well to the data obtained in the same experiment by the gas chromatograph method and to the results of previous measurements. An approximately the same but much less pronounced effect was also observed on the gas mass-spectrometer. If the gas sample was taken from the setup in several days after an electric explosion, we observed no electronegative effect, and the deuterium-to-hydrogen atomic ratio was approximately 1 : 1, which agrees fairly well with our hypothesis. Now, relying on the available data we unfortunately find it difficult to unambiguously interpret the observed effect. It should be noted that such a time-dependent effect was also observed by Santilli [14] who investigated the optical gas spectrum obtained during an electric arc ignition in a water-hydrocarbon mixture.

Therefore, the fact that both the methods had in the end a semi-quantitative character was determined not so much by the properties of the methods themselves as the properties of the gas mixture investigated. But hydrogen was nevertheless registered rather reliably in these experiments, which is a fairly strong argument in favour of the nuclear mechanism of hydrogen origin.

As has been said above, the method of partial hydrogen pressure measurement in a gas-collecting chamber made permanent long-term measurements possible. Figure 11 gives a typical example of measurements carried out within five days after electric explosion. The size of the squares in this figure corresponds to the error corridor in the hydrogen percentage measurements. The rhombs show errors in the measurement of the resultant gas-mixture pressure in the chamber. The setup was situated in a room whose daily temperature variations did not affect the measurement accuracy. The figure clearly demonstrates that the resultant pressure somewhat falls with time (most likely
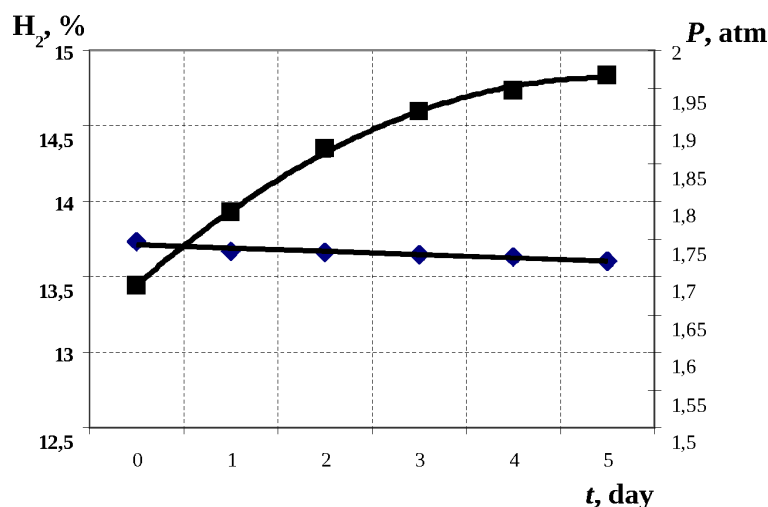
Fig. 11. Time dependence of partial hydrogen pressure. Squares – percentage of hydrogen; rhombuses – pressure in the chamber.

because of insufficient hermiticity), while the hydrogen percentage increases. The observed increase in the hydrogen percentage cannot be explained by the instrumental effect (e. g., by a gradual saturation of the hydrogen sensor) because the measurement was multiply repeated using gas chromatograph, and the results were coincident. The desire, of course purely intuitive, arises to relate the above-said fact to the previous one, but unfortunately there are no sufficient experimental grounds for establishing such a relationship.

To make the picture of the phenomenon objective, we decided to give here the results of our previous research works, which can relate to the experimental facts presented here but were published in scientific issues difficult to access, especially abroad. In the study of powder produced in a titanium foil explosion, attention was paid to the fact that part of the titanium powder is flowing on the surface of water that remained after the electric explosion. Since the titanium density is well known to be higher than that of water, this observation caused perplexity. With a special strainer the samples were collected and put under a scanning electron microscope DSM-960. The results obtained using the electron microscope are given in Figure 12. These photographs demonstrate that the particles flowing on the water surface are hollow. We deliberately destroyed the particle demonstrated in Figure 12a with thin tweezers, while in the particle in Figure 12b the hole was due to the high internal pressure in the course of its growth.

Then the hollow particles together with other foil remainders were examined for contained gases by the method described in detail in Section 4.3.1 of the present paper. For this purpose, the powder was dried, poured into the crucible, carefully weighed, and placed into the measuring volume, after which it was pumped out very slowly to avoid a sharp pressure drop and powder ejection from the crucible. After that the heating procedure was performed as described above. But as distinct from the background measurements, the pressure of the gas released in the accumulative volume was stabilized at a level of 0.2 Torr.

After pumping-out of the measuring volume, the powder-filled crucible was heated again. The heater power was raised to 750 W. When the heater power was maximum, the pressure only rose to 5×10^{-3} Torr, which testified to the absence of release of a considerable amount of hydrogen.

Then the next portion of powder underwent exactly the same procedure. The averaged results of measurements are given in the third row of Table 4. The released amount of hydrogen was $(4.6 \pm 0.9) \times 10^{20}$ molecules of H_2 per gram of powder, which is $\sim$ 50 times larger than in the original titanium foil. Thus, our measurements imply that the gas contained in the investigated powder is hydrogen by 95 %.

With allowance for the above results we can seek explanation of the increase in hydrogen concentration with time in either the hydrogen diffusion through thin walls of titanium spheres (Fig. 12a) or in degasification of hydrogen-saturated powder, or an unknown to us nuclear process which proceeded with characteristic half-life after an electric explosion. Based on the data available we cannot give preference to one partic-
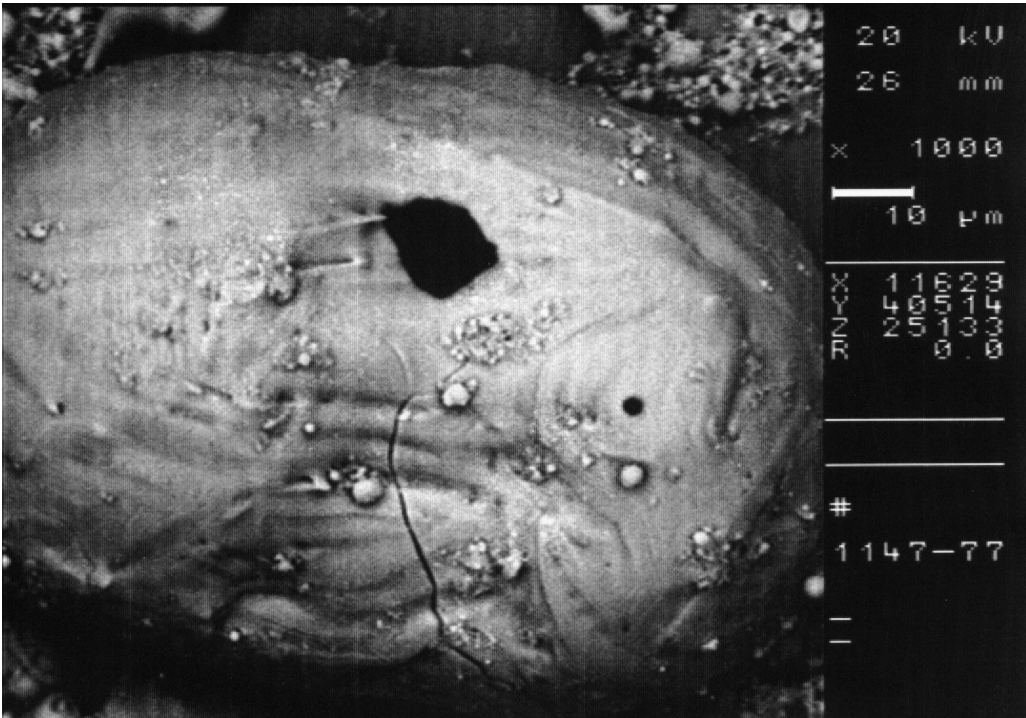
(a)
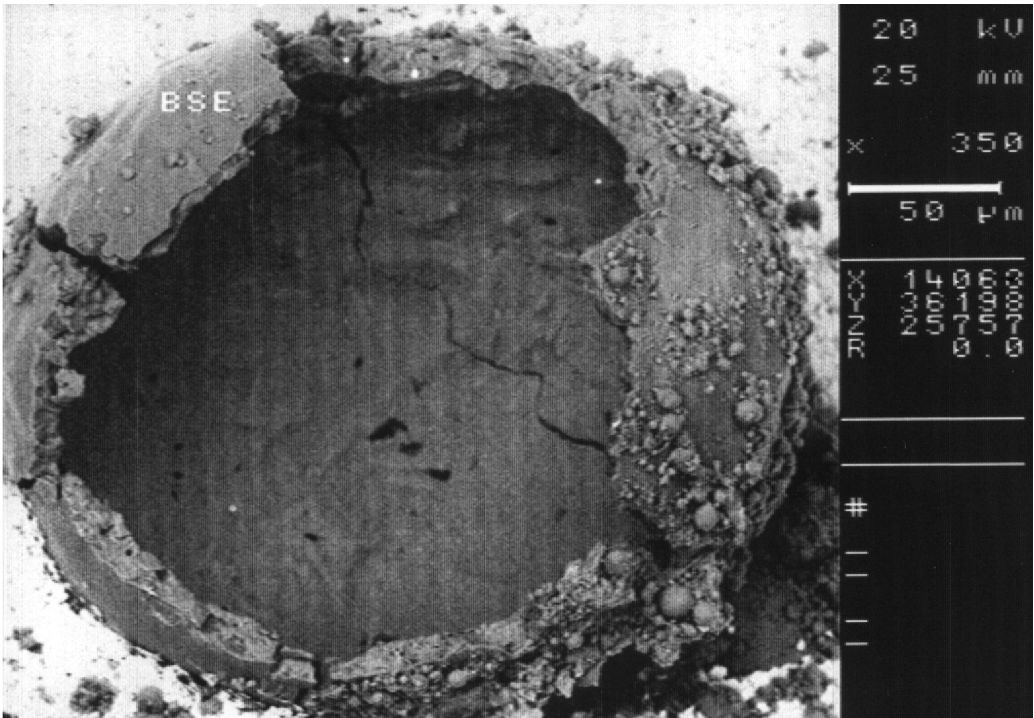
(b)

Fig. 12. Electron microscopic photographs of individual particles.

ular mechanism out of those discussed above. Further studies are needed. But proceeding from the fact of titanium powder 'hydrogenation' we can state that the bulk hydrogen is produced in the plasma channel at the moment of electric explosion.

5. Discussion

1. We have reliably established that an electric explosion of titanium foil in water induces production of a considerable amount of molecular hydrogen ($N_{H2} \sim 2 \times 10^{22}$ molecules). The origin of about half of this amount cannot be explained by water decomposition.

2. Careful search of the 'impurity' hydrogen source was not crowned with success.

3. The authors advanced a hypothesis on the nuclear mechanism of the origin of observed molecular hydrogen and obtained some results to back up the hypothesis.

We should emphasize that by the words 'nuclear mechanism' we of course mean neither the nuclear fission nor the nuclear fusion mechanism, at least in their traditional sense. The temperature of plasma produced upon electric explosion is too low (it is close to the solar corona temperature [10]), and such class of nuclear reactions is impossible in the present experiments. At the same time, on the basis of our preceding experiments [10, 15] we believe that in conditions of dense low-temperature nonequilibrium plasma, an absolutely new class of nuclear reactions may proceed in the absence of strong interactions. The main difference between the hypothetic nuclear reactions from the generally known ones is the assumption concerning their collective mechanism of interaction. We should notice that in plasma physics the role of collective interactions has long been thoroughly investigated and is beyond question, whereas in nuclear physics such a hypothesis seems to be very extravagant.

And nevertheless we elaborated [15] a phenomenological model of such hypothetic phenomenon based on i) the requirement of obeying the principal laws of conservation (of energy and baryon, lepton, and electric charges) and ii) computer simulation using the fact of finiteness (~ 300) of isotopes of stable nuclei. The predictions of the phenomenological model were verified experimentally [15]. The model suggests that if the titanium foil explosion proceeds in vanadium salt, ^{57}Fe nuclei must appear. Since ^{57}Fe isotope is rather rare in nature (its percentage in the iron isotope mixture is only $\sim 2.2\%$), its enrichment in the isotope mixture can readily be measured. Such experiments were carried out, and the model predictions were confirmed (for more details see [15]). The phenomenological model does not of course contain any assumptions concerning nuclear reaction mechanisms and is of prohibitive rather than predictive character.

Consistency with the conservation laws cannot serve as a sufficient condition for a real (observable) existence of collective nuclear reaction mechanism. Therefore, to describe such a mechanism it is necessary that any essentially new object be introduced into the basis of our fundamental representations. Taking into account the results of experimental studies [10, 11, 15 – 17] the authors think it is possible that a light lepton magnetic monopole, predicted theoretically by G. Lochak [18] can exist in nature. Lochak's magnetic monopole is something like the magnetically excited neutrino state. The possible mechanism of the described magnetic particle production due to electromagnetic symmetry breaking and their relation to the Standard Model were studied by H. Stumpf [19]. Examination of a possible magnetic monopole participation in the hydrogen production mechanism is not the goal of our present paper. However, application of such a hypothesis would allow a logically simple explanation of gas-mixture physical property variations in time. But additional research is needed for a strict scientific substantiation of such a hypothesis.

6. Conclusion

It is significant that although our results of relative hydrogen and deuterium content measurements seem to be reliable, in our opinion they cannot underlie the final conclusion concerning the nuclear origin of the observed hydrogen. The final conclusion will require additional research. However, the probability is much higher that the hydrogen described in our experiments has nuclear rather than chemical origin caused by some disregarded chemical processes.

[1] W. G. Chace and H. K. Moore (Eds.), Exploding wires, Plenum Press, New York 1962.

[2] Yu. Bakshaev, P. I. Blinov, A. S. Chernenko, S. A. Danko, Yu. G. Kalinin, V. D. Korolev, V. I. Tumanov, A. Yu. Shashkov, A. V. Chesnokov, and M. I. Ivanov, Plasma Phys. Rep. **27**, 1039 (2001); A. L. Velikovich, J. G. Wouchuk, C. Huete Ruiz de Lira, N. Metzler, S. Zalesak, and A. J. Schmitt, Phys. Plasmas **14**, 022706 (2007).

[3] L. I. Urutskoev and D. V. Filippov, Physics-Uspekhi **47**, 1257 (2004).

[4] F. Bosch, T. Faestermann, J. Friese, F. Heine, P. Kienle, E. Wefers, K. Zeitelhack, K. Beckert, B. Franzke, O. Klepper, C. Kozhuharov, G. Menzel, R. Mosham-mer, F. Nolden, H. Reich, B. Schlitt, M. Steck, T. Stöhlker, T. Winkler, and K. Takahashi, Phys. Rev. Lett. **77**, 5190 (1996).

[5] M. Jung, F. Bosch, K. Beckert, H. Eickhoff, H. Fol-ger, B. Franzke, A. Gruber, P. Kienle, O. Klepper, W. Koenig, C. Kozhuharov, R. Mann, R. Moshammer, F. Nolden, U. Schaaf, G. Soff, P. Spädtke, M. Steck, Th. Stöhlker, and K. Sm̈merer, Phys. Rev. Lett. **69**, 2164 (1992).

[6] D. V. Filippov, Phys. Atomic Nuclei **70**, 258; 2016 (2007).

[7] V. A. Erma, Phys. Rev. **105**, 1784 (1957).

[8] A. A. Sokolov, I. M. Ternov, and V. Ch. Zukovskii, Quantum Mechanics, Nauka, Moscow 1979.

[9] B. B. Kadomtsev and V. S. Kudryavtsev, JETP Lett. **13**, 61 (1971).

[10] L. I. Urutskoev, V. I. Liksonov, and V. G. Tsinoev, Ann. Fond. L.de Broglie **27**, 701 (2002).

[11] A. G. Volkovich, A. P. Govorun, A. A. Gulyaev, S. V. Zhukov, V. L. Kuznetsov, A. A. Rukhadze, A. V. Ste-blevskii, and L. I. Urutskoev, Ann. Fond. L. de Broglie **30**, 63 (2005).

[12] www.insovt.ru

[13] V. M. Dorovskoj, L. A. Elesin, V. L. Stolyarov, A. V. Steblevskij, L. I. Urutskoev, and D. V. Filippov, Prik-ladnaya fizika, **4**, 28 (2006) [in Russian].

[14] R. M. Santilli, Foundations of Hadronic Chemistry. With Applications to New Clean Energies and Fu-els, Kluwer Academic Publishers, Boston-Dordrecht-London 2001.

[15] D. V. Filippov and L. I. Urutskoev, Ann. Fond. L. de Broglie **29**, Hors Serie 3, 1187 (2004).

[16] N. G. Ivoilov and L. I. Urutskoev, Ann. Fond. L. de Broglie **29**, Hors Serie 3, 1177 (2004).

[17] D. Priem, G. Racineux, G. Lochak, C. Daviau, D. Far-gue, M. Karatchentzeff, and H. Lehn, Ann. Fond. L. de Broglie **33**, 129 (2008).

[18] G. Lochak, Z. Naturforsch. **62a**, 231 (2007); T. W. Bar-ret and D. M. Grimes (Eds.), in Advanced Electromag-netism World Scientific, Singapore 1995, p. 105.

[19] H. Stumpf, Z. Naturforsch. **60a**, 696 (2005); **61a**, 439 (2006).